(4)

DTIC FILE COPY

CHEMICAL
RESEARCH,
DEVELOPMENT &
ENGINEERING
CENTER

AD-A191 479

CRDEC-CR-88020

SIMULATIONS OF A MISSILE WITH LIQUID PAYLOAD UNDER LAUNCH CONDITIONS

by Simon Rosenblat

FLUID DYNAMICS
INTERNATIONAL, INCORPORATED
Evanston, IL 60201

January 1988

U.S. ARMY
ARMAMENT
MUNITIONS
CHEMICAL COMMAND

Aberdeen Proving Ground, Maryland 21010-5423

Disclaimer

The findings in this report are not to be construed as an official Department of the Army position unless so designated by other authorizing documents.

Distribution Statement

Approved for public release; distribution is unlimited.

REPORT DOCUMENTATION PAGE

1a. REPORT SECURITY CLASSIFICATION UNCLASSIFIED	1b. RESTRICTIVE MARKINGS
2a. SECURITY CLASSIFICATION AUTHORITY 2b. DECLASSIFICATION / DOWNGRADING SCHEDULE	3. DISTRIBUTION / AVAILABILITY OF REPORT Approved for public release; distribution is unlimited.
4. PERFORMING ORGANIZATION REPORT NUMBER(S) CRDEC-CR-88020	5. MONITORING ORGANIZATION REPORT NUMBER(S)
6a. NAME OF PERFORMING ORGANIZATION Fluid Dynamics International, Incorporated 6b. OFFICE SYMBOL (If applicable)	7a. NAME OF MONITORING ORGANIZATION
6c. ADDRESS (City, State, and ZIP Code) Suite 400 1600 Orrington Avenue Evanston, IL 60201	7b. ADDRESS (City, State, and ZIP Code)
8a. NAME OF FUNDING / SPONSORING ORGANIZATION CRDEC 8b. OFFICE SYMBOL (If applicable) SMCCR-RSP-A	9. PROCUREMENT INSTRUMENT IDENTIFICATION NUMBER DAAD05-86-M-Q985
8c. ADDRESS (City, State, and ZIP Code) Aberdeen Proving Ground, MD 21010-5423	10. SOURCE OF FUNDING NUMBERS PROGRAM ELEMENT NO / PROJECT NO / TASK NO / WORK UNIT ACCESSION NO

11. TITLE (Include Security Classification)
Simulations of a Missile with Liquid Payload Under Launch Conditions

12. PERSONAL AUTHOR(S)
Rosenblat, Simon

13a. TYPE OF REPORT	13b. TIME COVERED	14. DATE OF REPORT (Year, Month, Day)	15. PAGE COUNT
Contractor	FROM 86 Sep TO 87 Sep	1988 January	32

16. SUPPLEMENTARY NOTATION
COR: Daniel Weber, SMCCR-RSP-A, (301) 671-2186

17. COSATI CODES			18. SUBJECT TERMS (Continue on reverse if necessary and identify by block number)
FIELD	GROUP	SUB-GROUP	Liquid Payloads; Newtonian Fluid; Computational Fluid Dynamics; Non-Newtonian Fluid; Finite Elements
15	06	03	

19. ABSTRACT (Continue on reverse if necessary and identify by block number)

A numerical simulation of the flow of a liquid in the annular region between two coaxial circular cylinders was performed. This simulation corresponds to the actual behavior of a missile with a liquid payload during its launch phase. The simulation was performed in two parts. The first part was to determine if the payload liquid, which comprised both Newtonian and non-Newtonian fluids, would achieve full spin up relative to the missile during launch. During the second part, the despin moments acting on the spinning and nutating missile with a fully spun up liquid payload were determined from the steady-state Navier-Stokes equations relative to an aeroballistic reference frame. The simulations were performed with a finite element software package FIDAP. The majority of the computations were done on an HP9000 minicomputer; some were done on a Microvax workstation.

20. DISTRIBUTION / AVAILABILITY OF ABSTRACT ☒ UNCLASSIFIED/UNLIMITED ☐ SAME AS RPT ☐ DTIC USERS	21. ABSTRACT SECURITY CLASSIFICATION UNCLASSIFIED
22a. NAME OF RESPONSIBLE INDIVIDUAL SANDRA J. JOHNSON	22b. TELEPHONE (Include Area Code) (301) 671-2914 22c. OFFICE SYMBOL SMCCR-SPS-T

DD FORM 1473, 84 MAR — 83 APR edition may be used until exhausted. All other editions are obsolete.

PREFACE

The work described in this report was authorized under Contract No. DAAD05-86-M-Q985. This work was started in September 1986 and completed in September 1987.

The use of trade names or manufacturers' names in this report does not constitute an official endorsement of any commercial products. This report may not be cited for purposes of advertisement.

This report has been approved for release to the public.

Blank

CONTENTS

	Page
INTRODUCTION	7
Part I - SPIN UP	8
Part II - DESPIN MOMENT	29

Blank

SIMULATIONS OF A MISSILE WITH LIQUID PAYLOAD UNDER LAUNCH CONDITIONS

INTRODUCTION

This project was concerned with the numerical simulation of the flow of a liquid in the annular region between two coaxial circular cylinders. The investigations related to the behavior of a missile with a liquid payload during and immediately following launch.

The project comprised two Parts. In Part 1 solutions were computed of the transient Navier-Stokes equations for a number of different liquids, both Newtonian and non-Newtonian, with the object of determining whether or not the liquid became fully spun up over a given interval of time. In Part II the steady-state Navier-Stokes equations relative to an aeroballistic frame were solved with the aim of determining the despin moment on a spinning and nutating missile in a fully-spun-up mode.

Detailed descriptions of the two problems will be given below. In both Parts the simulations were performed with the finite element software package FIDAP. Most of the computations were done on an HP 9000 mini-computer; some were done on a Microvax workstation.

Part I

SPIN UP

Formulation

Computations were performed to determine the spin up characteristics of a number of different liquids, both Newtonian and non-Newtonian, under conditions simulating the launch of a missile with a liquid payload. The essential features of the process studied were:

i. the time interval over which spin up took place was from 0.01 sec to 0.12 sec;

ii. the spin rate was accelerated over this time interval in a prescribed manner (detailed below) from zero to 11.8 rev/sec.

iii. the axial acceleration varied over the same time interval in a prescribed manner (detailed below), with a value of 585 m/sec^2 at the end of the interval.

The liquid was taken to occupy the region between two coaxial circular cylinders of radii

$$R_1 = 2.625'' \ , \ R_2 = 4.5''$$

respectively. The boundaries of the annular region were rigid and the length of the cylinders was 66". However, the liquid filled only 70% of the region, so that the effective (mean) length of the liquid column was

$$d = 46.2''.$$

The equations governing the motion of the liquid are the Navier-Stokes equations and the continuity equation, which can be written as

$$\rho(\underline{v}^*_{t^*} + \underline{v}^* \cdot \nabla^* \underline{v}^*) = -\nabla^* p^* + \nabla^* \cdot \underline{\underline{T}}^* + \rho \underline{F}^* \qquad (1)$$

$$\nabla^* \cdot \underline{v}^* = 0 \qquad (2)$$

where ρ is the density, $\underline{v}^*$ is velocity, p^* is pressure, $\underline{T}^*$ is extra stress and $\underline{F}^*$ is a body force vector which depends on the time t^*. Associated with these equations is a constitutive relation between the stress tensor and the strain-rate tensor:

$$\underline{T}^* = \mu_o \, \underline{G}^* \, (\dot{\underline{\gamma}}^*) \tag{3}$$

where μ_o is zero-shear-rate viscosity and where

$$\dot{\underline{\gamma}}^* = \tfrac{1}{2}(\nabla^* \underline{v}^* + \nabla^* \underline{v}^{*T}). \tag{4}$$

For Newtonian liquids (3) is just a linear relation; for the non-Newtonian liquids studied $\underline{G}^*$ was given by empirical data.

Nondimensionalization

It is convenient to express the governing equations and associated quantities in nondimensional form. All lengths are scaled with respect to the outer radius R_2, time with respect to the final angular velocity ω (=11.8 rev/sec), and velocities with respect to the velocity $R_2\omega$. Thus we write

$$\underline{v}^* = R_2\omega\underline{v},\ t^* = \omega^{-1}t,\ \underline{r}^* = R_2\underline{r},\ p^* = \rho(R_2\omega)^2 p,$$
$$\underline{T}^* = \mu_o\omega\underline{T},\ \underline{F}^*(t^*) = R_2\omega^2\underline{F}(t),\ \dot{\underline{\gamma}}^* = \omega\dot{\underline{\gamma}}.$$

Then the governing equations (1) - (4) become

$$\underline{v}_t + \underline{v}\cdot\nabla\underline{v} = -\nabla p + \frac{1}{Re}\nabla\cdot\underline{T} + \underline{F}(t) \tag{5}$$

$$\nabla\cdot\underline{v} = 0 \tag{6}$$

with

$$\underline{T} = \underline{G}(\dot{\underline{\gamma}}) \tag{7}$$

and

$$\dot{\underline{\gamma}} = \tfrac{1}{2}(\nabla\underline{v} + \nabla\underline{v}^T) \tag{8}$$

The parameter appearing in equation (5) is the Reynolds number based on zero-shear-rate viscosity,

$$Re = \frac{\rho R_2^2 \omega}{\mu_o} \tag{9}$$

We now specify in more detail certain scalings used in the calculations. The final angular velocity is

$$\omega = 11.8 \text{ revs/sec} \quad = 74.14 \text{ rads/sec}$$

so that

$$\omega^{-1} = .0135 \text{ sec.}$$

The time of spin up is from $t^* = 0.01$ sec to $t^* = 0.12$ sec, and the spin rate increases linearly from $t^* = 0.01$ sec to $t^* = 0.08$ sec, and then is constant. We therefore define a dimensionless time t by the formula

$$t^* = .01 + .0135t$$

or, equivalently,

$$t = 74.14\ (t^* - .01).$$

The relation between dimensional and dimensionless spin up times is therefore as shown in the following table

t^*	t
.01	0.0000
.08	5.1900
.12	8.1554

Thus the total dimensionless spin up time is $t = 8.1554$.

We can also conveniently define a dimensionless angular velocity Ω which changes in time, as indicated above, as follows:

$$\Omega = \Omega(t) = \begin{cases} t/5.19 & \text{for } o \le t \le 5.19 \\ 1 & \text{for } 5.19 \le t \le 8.1554 \end{cases} \tag{10}$$

It is convenient also to non-dimensionalize the time-dependent body force. This increases until $t^* = 0.08$ and then experiences a small decrease. At the final instant $t^* = 0.12$ it is given that

$$F^*_{final} = 585.50 \text{ m/sec}^2.$$

When this is scaled with respect to $R_2\omega^2$ we obtain

$$F_{final} = F^*_{final}/R_2\omega^2 = 0.9319$$

Hence we write the dimensionless acceleration over the time interval of interest as

$$F(t) = -0.9319 f(t) \tag{11}$$

where

$$f(t) = \begin{cases} .1115 + .1790t & 0 \le t \le 5.19 \\ 1.1108 - 0.0136t & 5.19 \le t \le 8.1554 \end{cases} \tag{12}$$

The values at different times represented by (11) and (12) are indicated in the following table:

t	$f(t)$	$F(t)$	t^*	$F^*(t^*)$
0	.1115	− .1039	.01	− 65.28
5.19	1.0403	− .9695	.08	− 609.1
8.1554	1.0000	− .9319	.12	− 585.5

The simulations were performed for a total of 15 different liquids. Five were Newtonian and ten were non-Newtonian. For identification purposes

the ten non-Newtonian liquids were labeled liquid 1, liquid 2,...,liquid 10. The Newtonian liquids were labeled liquid 1*N*, liquid 2*N*, liquid 5*N*, liquid 6*N* and liquid 8*N*. This was because of equality between the viscosity of liquid 1*N* with the zero-shear-rate viscosity of liquid 1, etc. These viscosities and the corresponding Reynolds numbers are shown in Table 1. The dependence of the non-Newtonian liquids' viscosities on shear rate was determined from empirical data supplied.

liquid #	μ_0 poise	*Re*
1	1000	9.688
1*N*	1000	9.688
2	600	16.15
2*N*	600	16.15
3	380	25.50
4	200	48.44
5	100	96.88
5*N*	100	96.88
6	60	161.5
6*N*	60	161.5
7	20	484.4
8	10	968.8
8*N*	10	968.8
9	6	1615
10	2	4844

TABLE 1. Liquids and zero-shear-rate viscosities

Initial and Boundary Conditions

The initial conditions for the simulation were that the liquid was at rest at (dimensionless) time $t = 0$.

The boundary conditions are applied to all the surfaces. The inner and outer curved boundaries are at dimensionless radial positions 0.5833 and 1.0 respectively. The lower, solid end boundary of the cylinder is at $z = 0$ in a cylindrical polar coordinate system, while the mean position of the upper free surface is at $z = 10.27$.

The boundary conditions are:

i. On the inner curved surface $r = 0.5833$, $0 < z < 10.27$,

$$u = w = 0 \ , \ v = 0.5833\,\Omega(t)$$

where $\Omega(t)$ is given by equation (10); (u,v,w) are the velocity components in the radial, azimuthal and axial directions respectively.

ii. On the outer curved surface $r = 1.0$, $0 < z < 10.27$,

$$u = w = 0 \ , \ v = 1.\Omega(t)$$

iii. On the base $z = 0$,

$$u = w = 0 \ , \ v = r\Omega(t) \ , \ 0.5833 < r < 1.0.$$

IV. On the upper free surface it is assumed that the surface tension is zero. The boundary conditions on this surface are then that the normal velocity is zero and that the tangential stress is zero. These translate into

$$w = \frac{\partial u}{\partial z} = \frac{\partial v}{\partial z} = 0$$

on the mean position $z = 10.27$.

Computations and Results

The problem was solved as a transient problem over the time interval

$0 < t < 8.1554$. Fixed time increments were used of length 0.02039, so that 40 time steps were required to complete the simulation. Each run took approximately 8 hours of c.p.u. time on an HP 9000 computer, except for liquids 9 and 10, where the run time became excessively long because of the need to design an extremely fine mesh.

The results are presented in the accompanying graphs. Figures 1-13 show the behavior of the azimuthal component of velocity at one particular point in the liquid as a function of time. This point was chosen (arbitrarily) to have a radial coordinate $r = 0.756$. The velocity at this point was zero at $t = 0$, and if the liquid is fully spun up into rigid body motion, it should have an azimuthal velocity $v = 0.756$ at the end of the time interval $t = 8.155$. The figures show that the Newtonian liquids $1N$ and $2N$ are indeed fully spun up, while none of the others is completely spun up. The non-Newtonian liquids 1 and 2 are nearly spun up, to within a few percent. The velocity at this point which is actually reached is a measure of the extent to which complete spin up has been achieved. Using the ratio of velocity attained to the spin up value (.756) as a simple measure, we can refer to percentages as shown in Table 2. Liquids 9 and 10 are so far from being spun up that the solutions were not calculated; they are in fact less than 1% spun up. Table 2 shows the dramatic decrease in the extent of spin up as viscosity decreases, as well as the significant effects of shear thinning.

liquid #	Percentage spin up
1	97
1*N*	100
2	95
2*N*	100
3	89
4	66
5	40
5*N*	92
6	26
6*N*	79
7	4
8	1
8*N*	11

TABLE 2. Percentage spin up

Figure 1

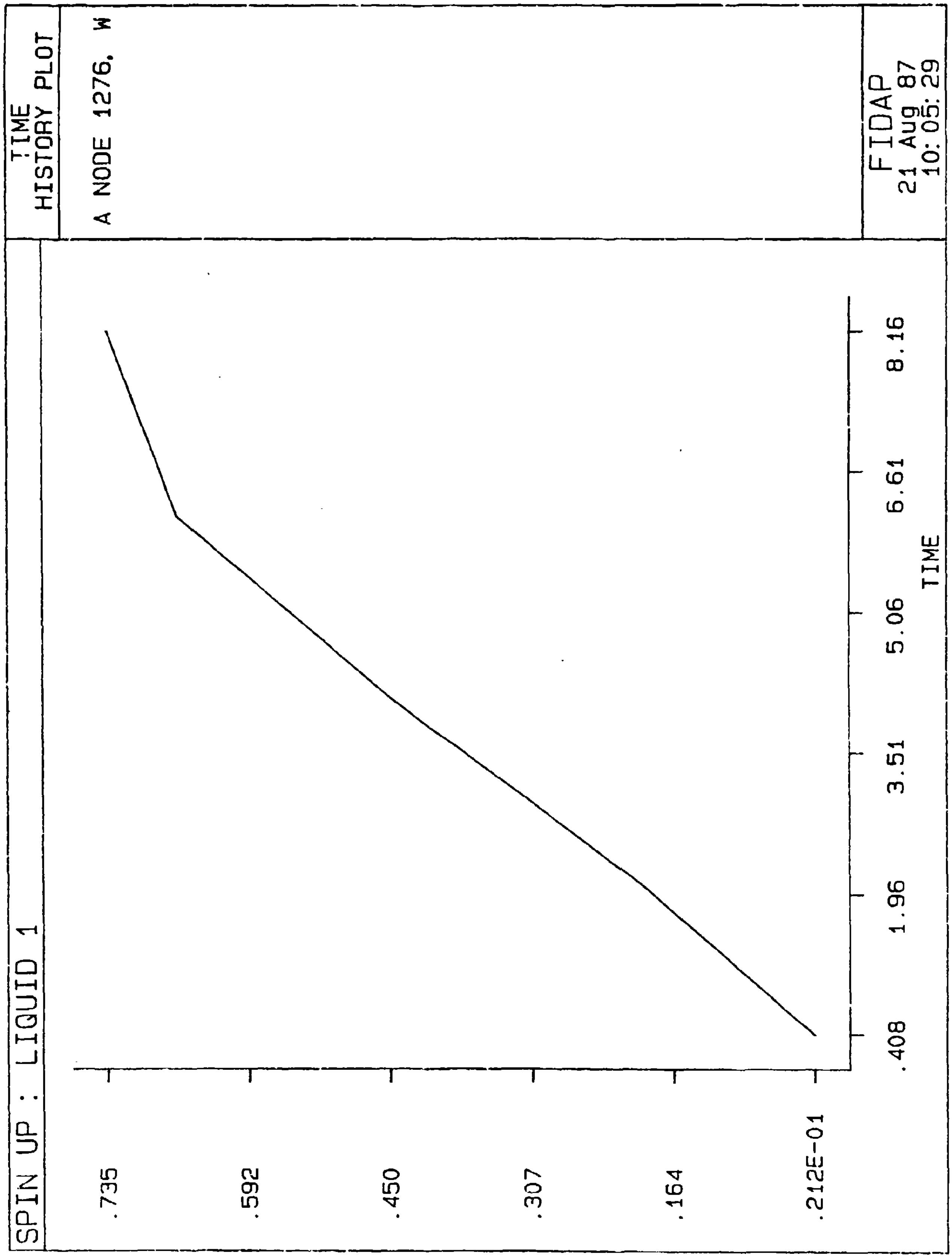
SPIN UP : LIQUID 1
TIME
HISTORY PLOT
A NODE 1276. W
FIDAP
21 Aug 87
10:05:29
.735
.592
.450
.307
.164
.212E-01
.408
1.96
3.51
5.06
6.61
8.16
TIME

Figure 2

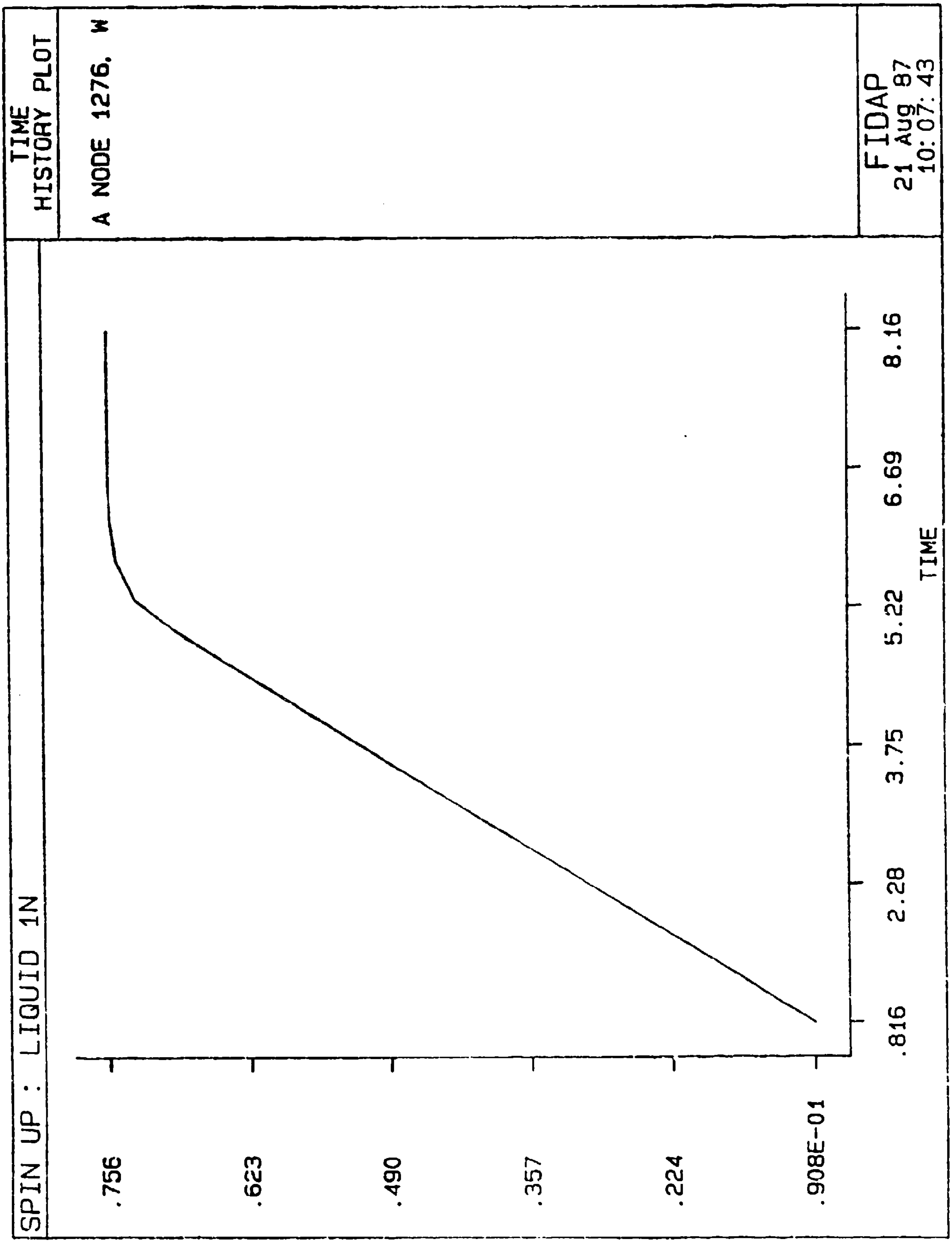
TIME
HISTORY PLOT
A NODE 1276. W
FIDAP
21 Aug 87
10:07:43
SPIN UP : LIQUID 1N
.756
.623
.490
.357
.224
.908E-01
.816
2.28
3.75
5.22
6.69
8.16
TIME

Figure 3

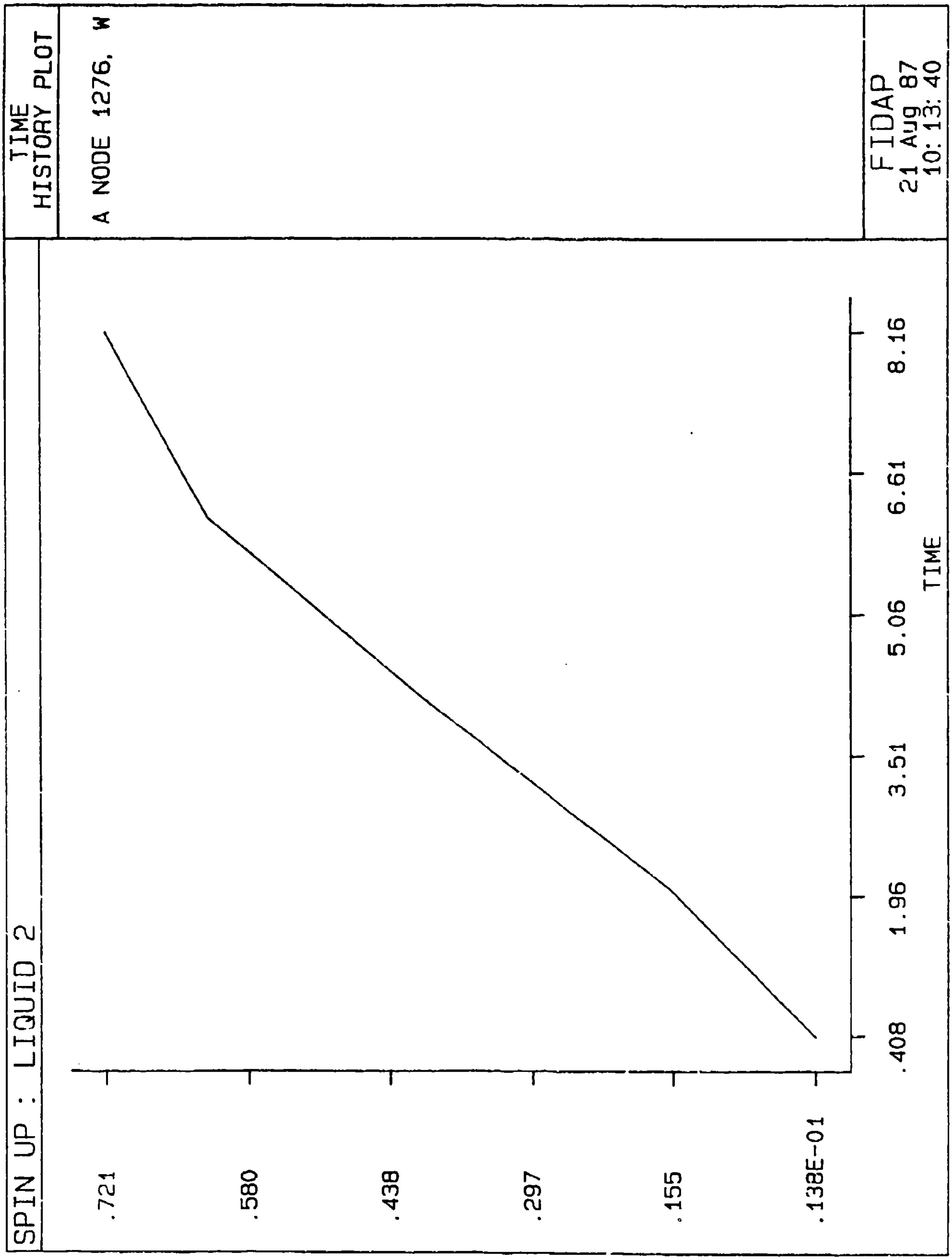

SPIN UP : LIQUID 2
TIME
HISTORY PLOT
A NODE 1276, W
FIDAP
21 Aug 87
10:13:40
.721
.580
.438
.297
.155
.138E-01
.408
1.96
3.51
5.06
6.61
8.16
TIME

Figure 4

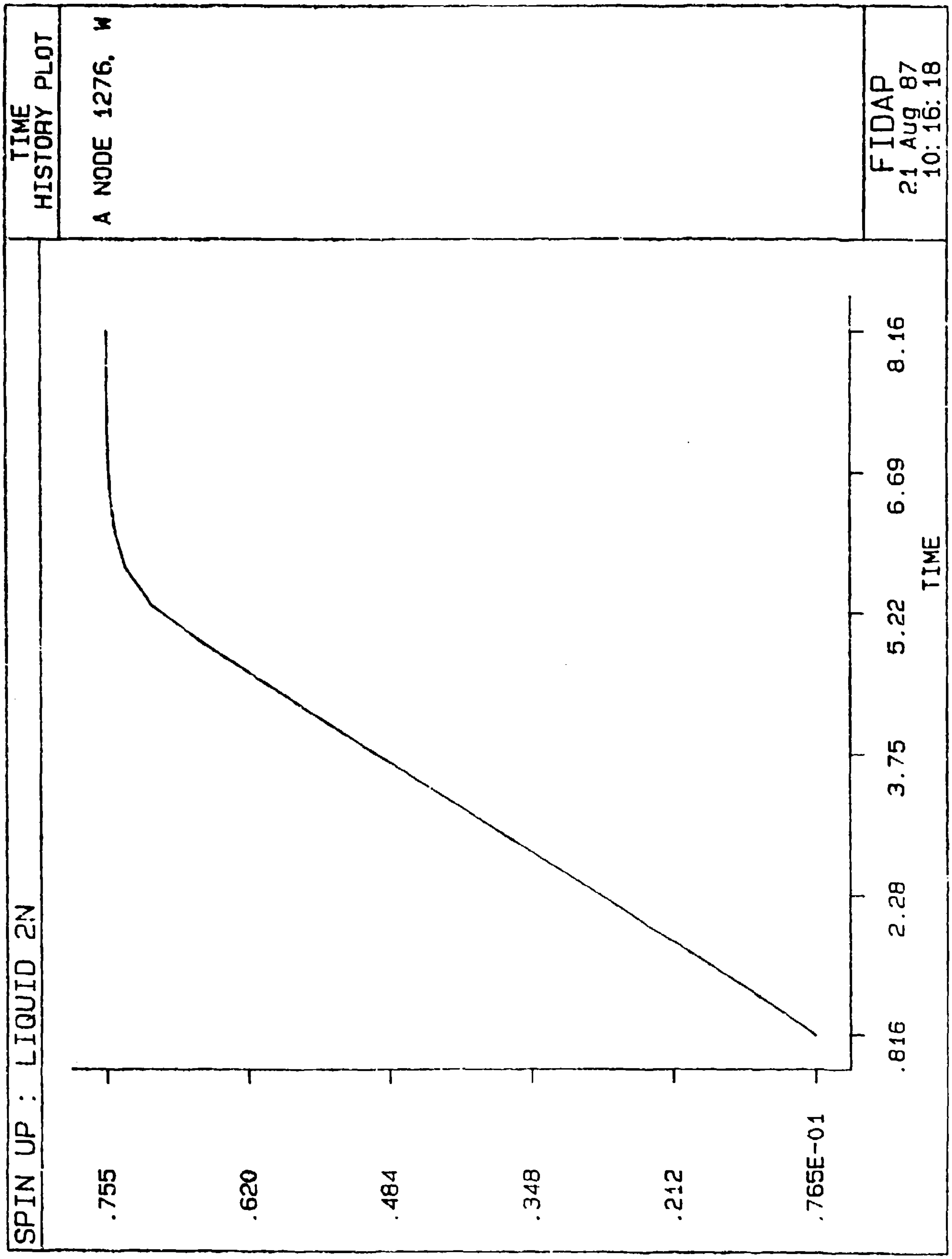
SPIN UP : LIQUID 2N
TIME
HISTORY PLOT
A NODE 1276, W
FIDAP
21 Aug 87
10:16:18
.755
.620
.484
.348
.212
.765E-01
.816
2.28
3.75
5.22
6.69
8.16
TIME

Figure 5

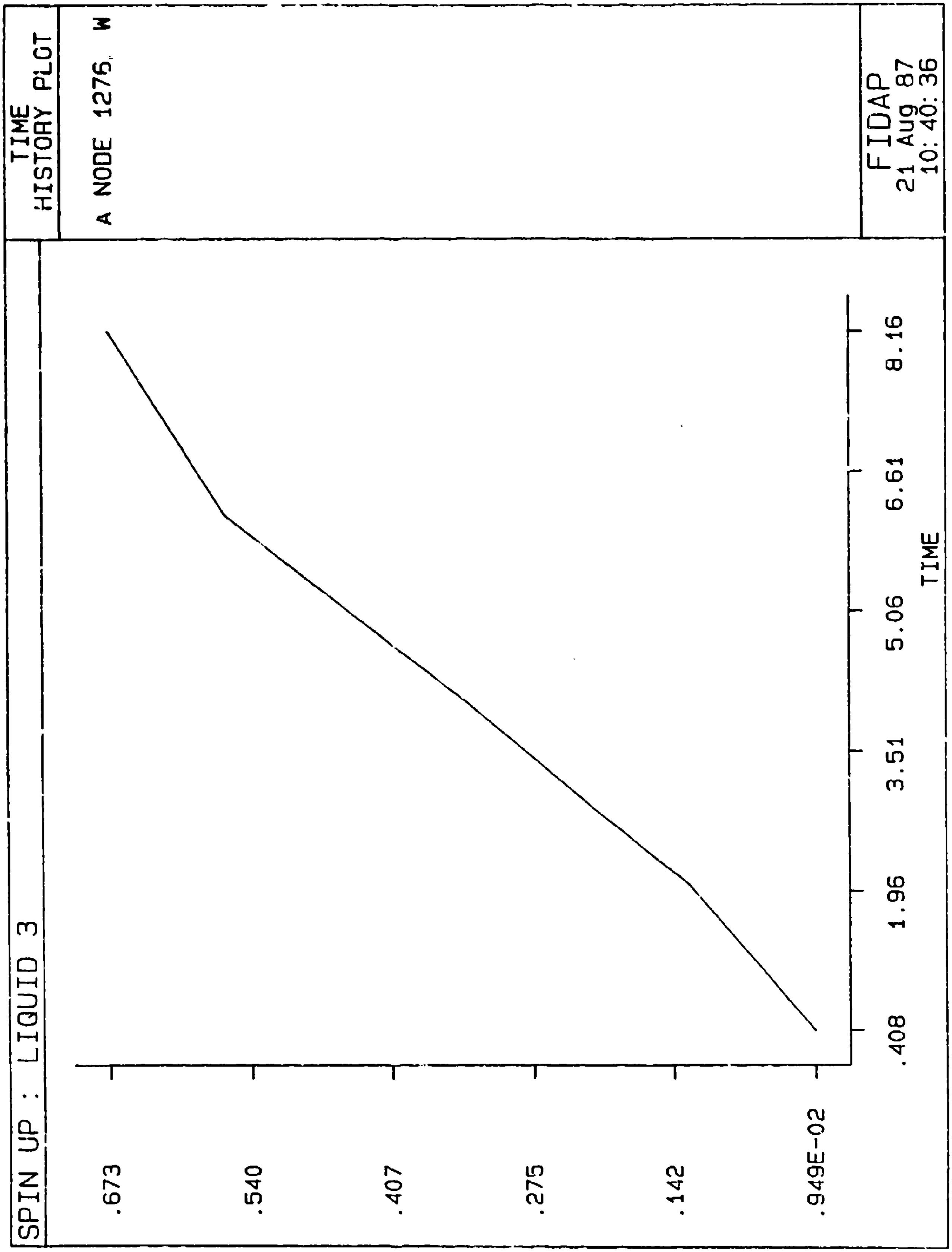
SPIN UP : LIQUID 3
TIME
HISTORY PLOT
A NODE 1276 W
FIDAP
21 Aug 87
10:40:36
.673
.540
.407
.275
.142
.949E-02
.408
1.96
3.51
5.06
6.61
8.16
TIME

Figure 6

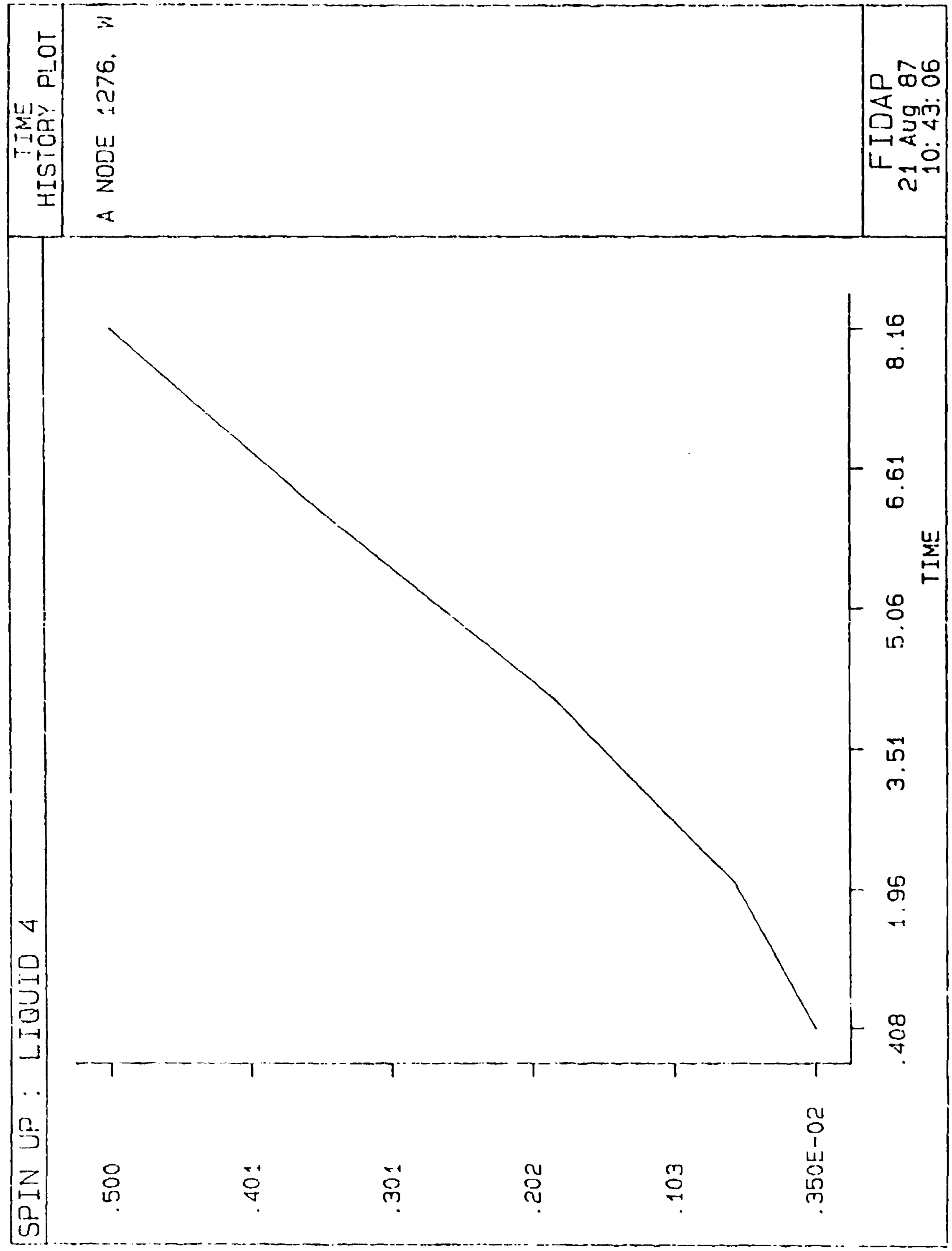
SPIN UP : LIQUID 4
TIME HISTORY PLOT
A NODE 1276, W
FIDAP
21 Aug 87
10:43:06
.500
.401
.301
.202
.103
.350E-02
.408
1.96
3.51
5.06
6.61
8.16
TIME

Figure 7

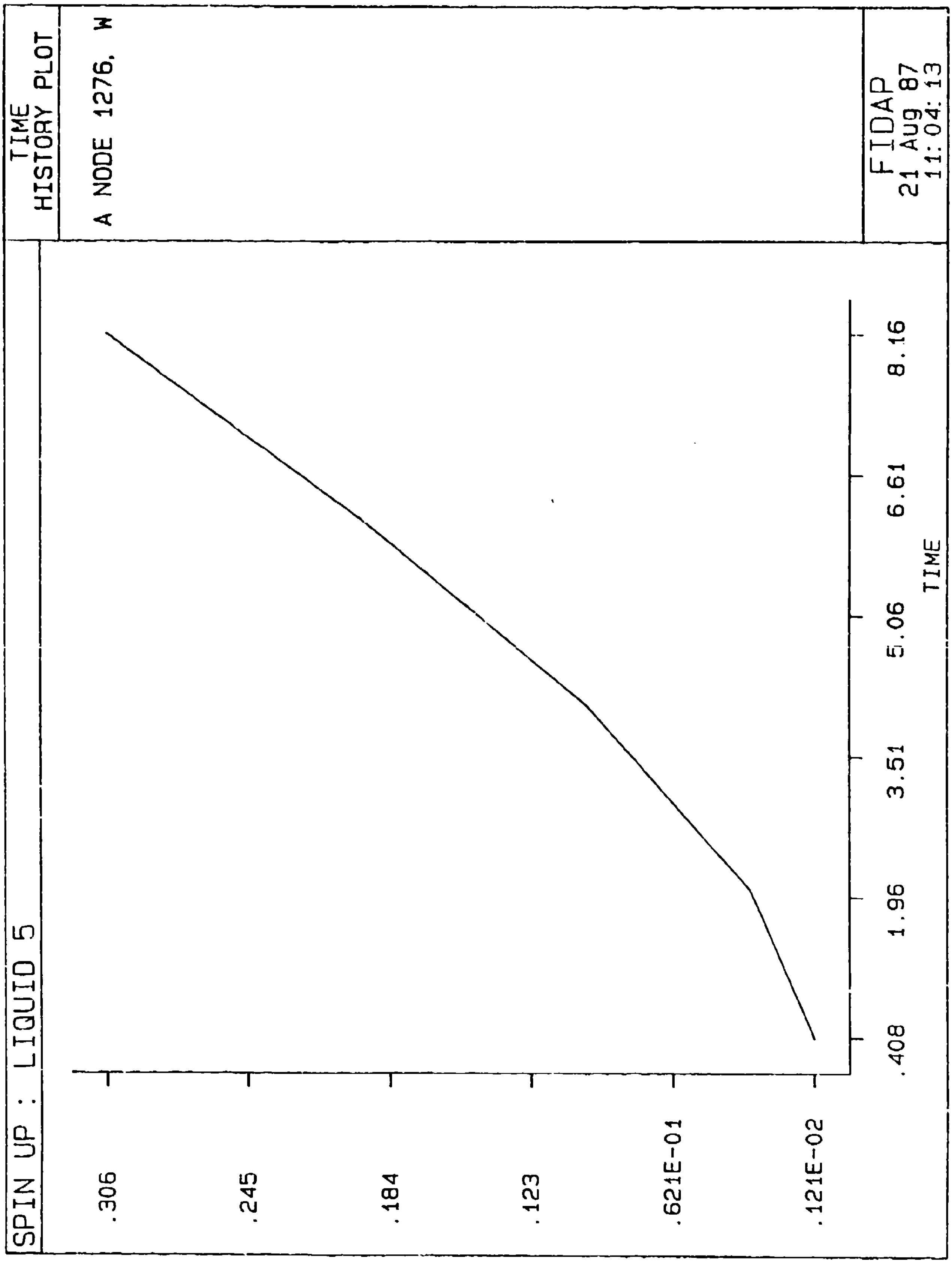

TIME
HISTORY PLOT
A NODE 1276, W
FIDAP
21 Aug 87
11:04:13
SPIN UP : LIQUID 5
.306
.245
.184
.123
.621E-01
.121E-02
.408
1.96
3.51
5.06
6.61
8.16
TIME

Figure 8

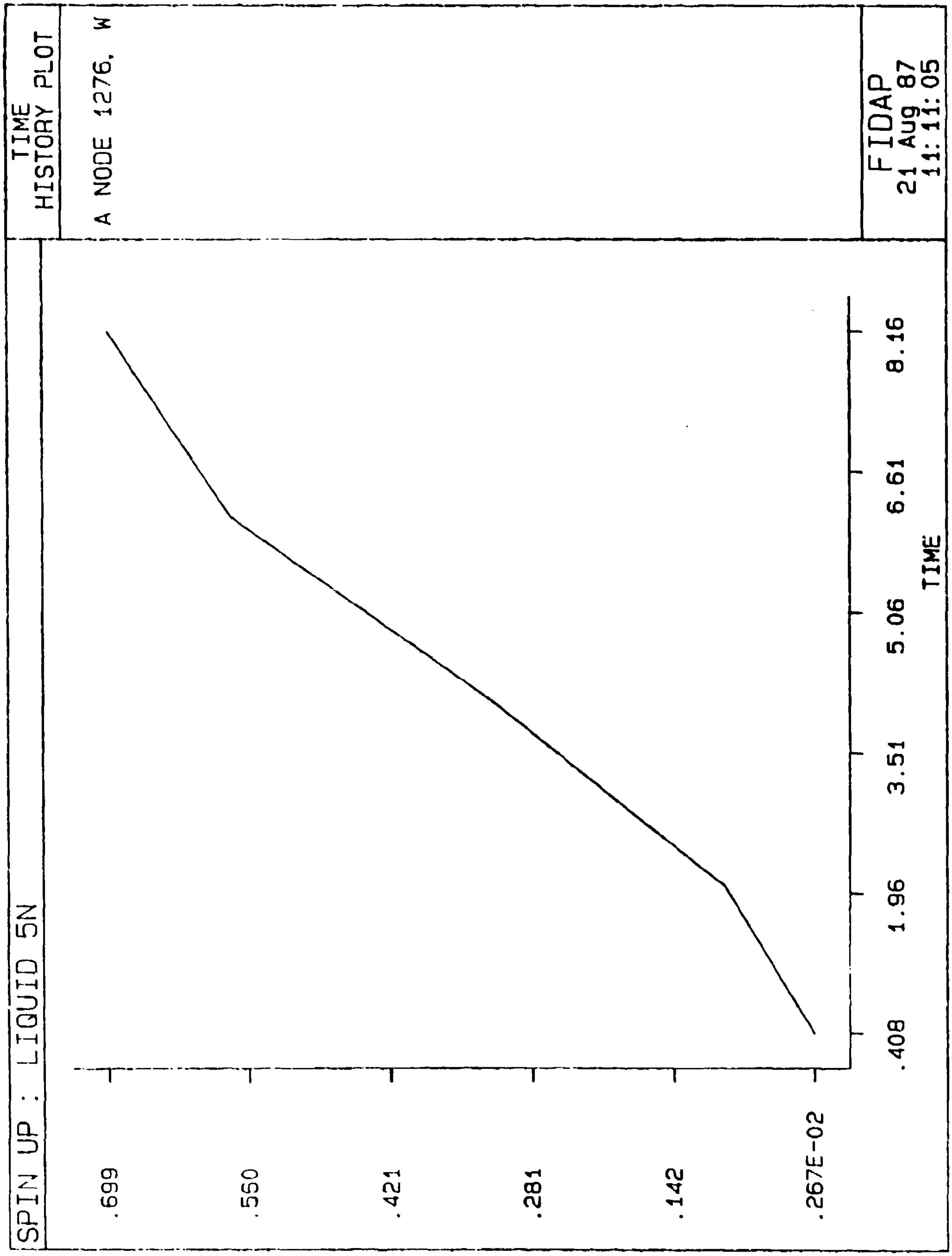
SPIN UP : LIQUID 5N
TIME
HISTORY PLOT
A NODE 1276, W
FIDAP
21 Aug 87
11:11:05
.699
.550
.421
.281
.142
.267E-02
.408
1.96
3.51
5.06
6.61
8.16
TIME

Figure 9

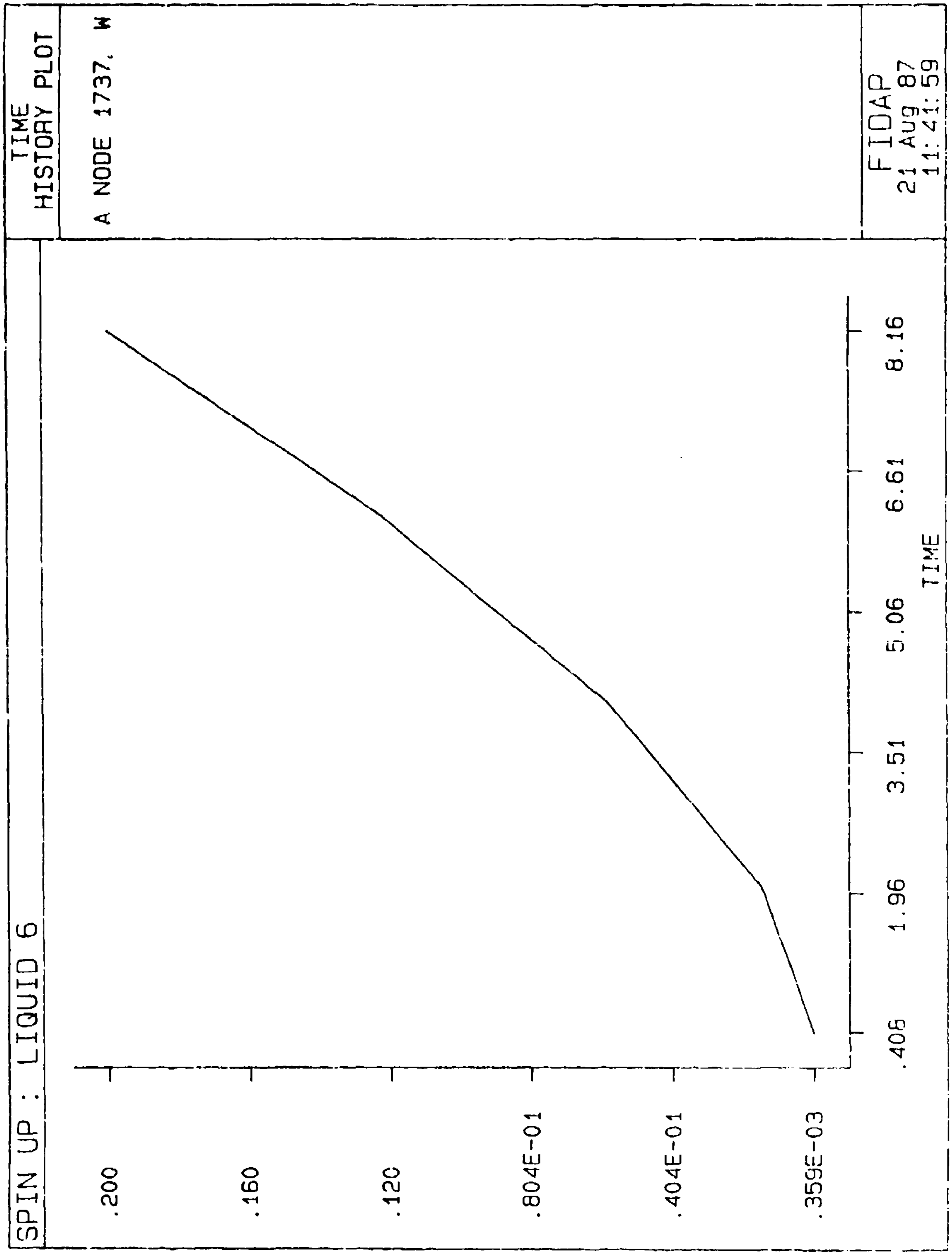

SPIN UP : LIQUID 6
TIME
HISTORY PLOT
A NODE 1737. W
FIDAP
21 Aug 87
11:41:59
.200
.160
.120
.804E-01
.404E-01
.359E-03
.408
1.96
3.51
5.06
6.61
8.16
TIME

Figure 10

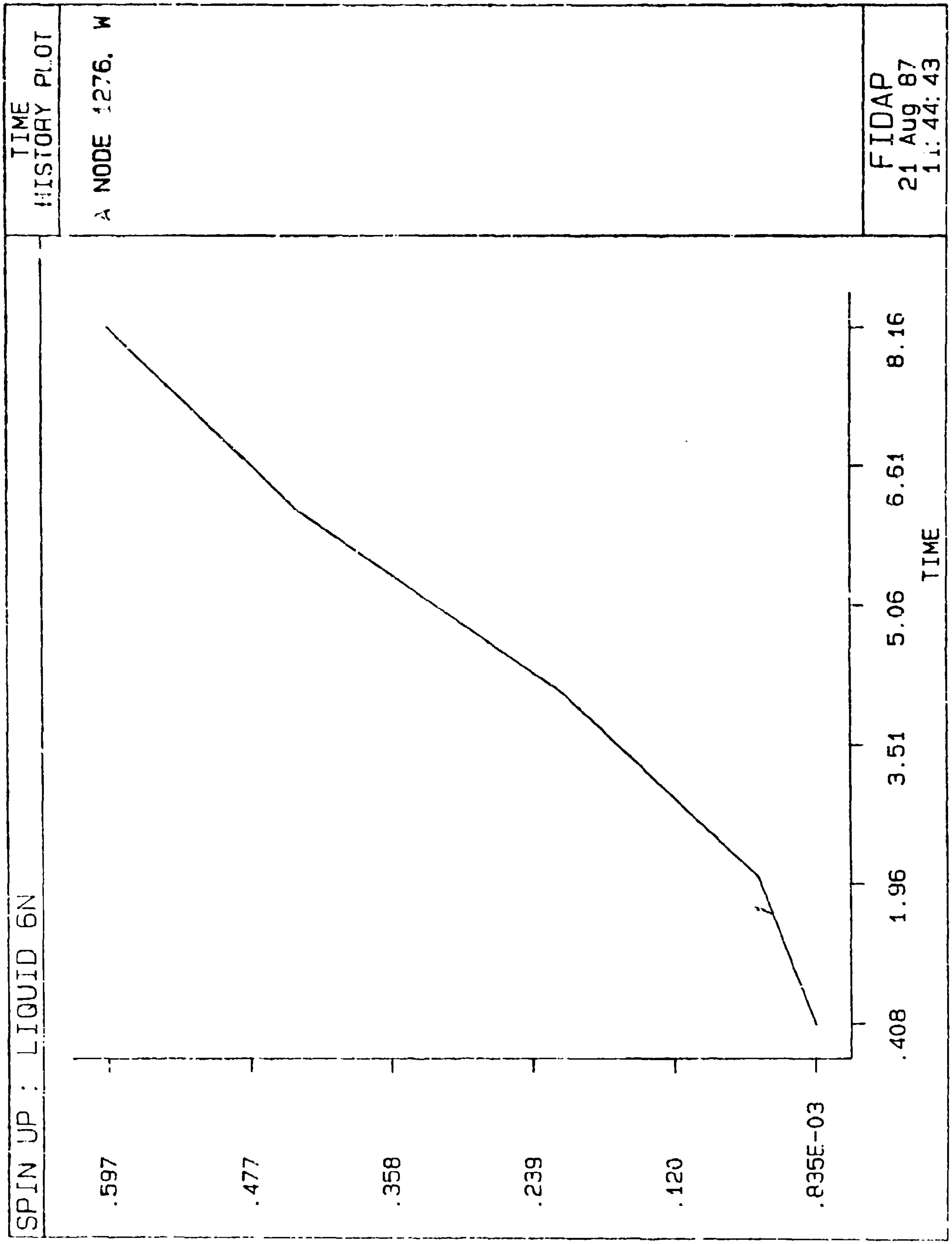
SPIN UP : LIQUID 6N
TIME
HISTORY PLOT
A NODE 1276. W
FIDAP
21 Aug 87
11:44:43
.597
.477
.358
.239
.120
.835E-03
.408
1.96
3.51
5.06
6.61
8.16
TIME

Figure 11

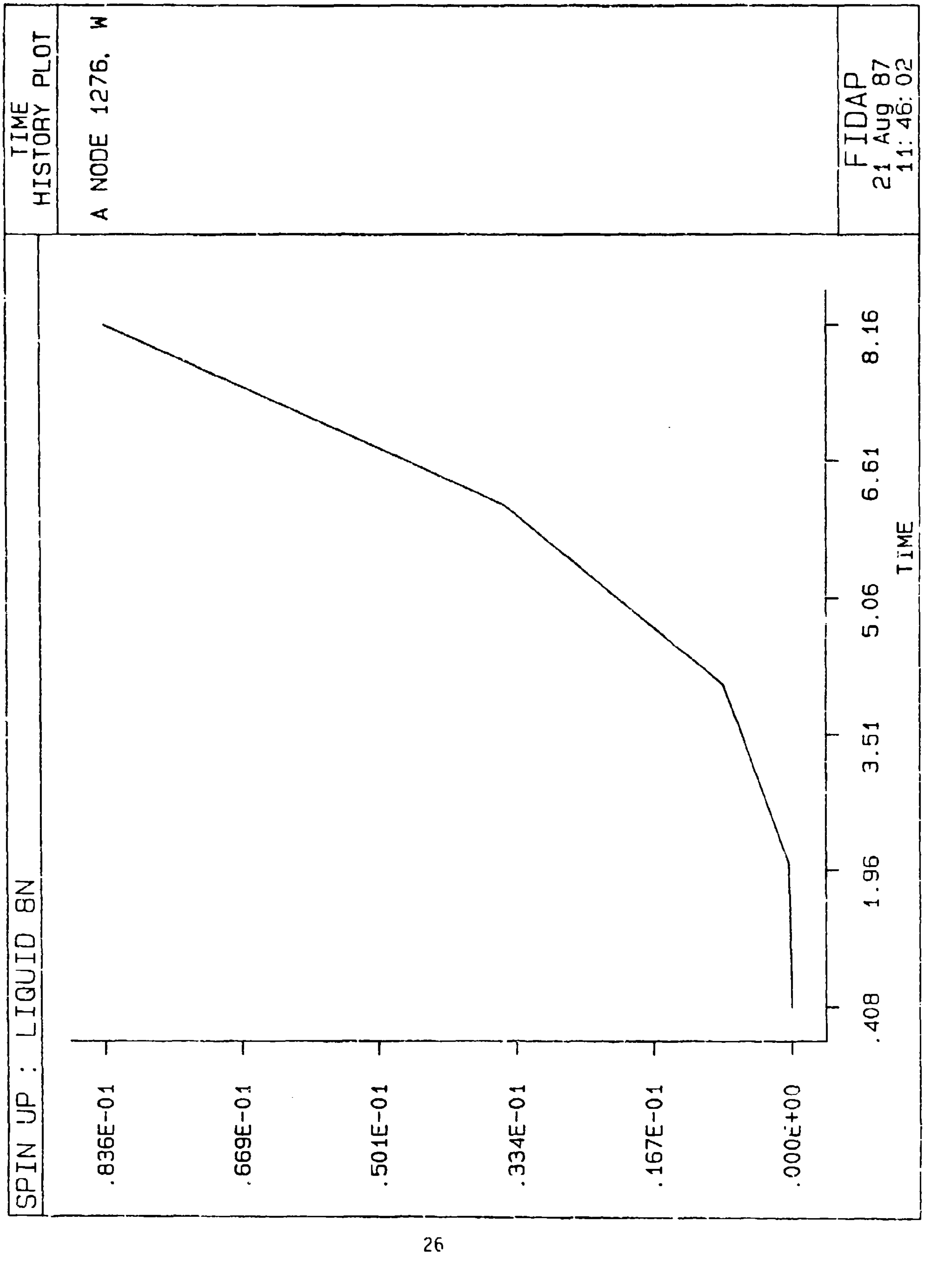

SPIN UP : LIQUID 8N
TIME
HISTORY PLOT
A NODE 1276. W
FIDAP
21 Aug 87
11:46:02
.836E-01
.669E-01
.501E-01
.334E-01
.167E-01
.000E+00
.408
1.96
3.51
5.06
6.61
8.16
TIME

Figure 12

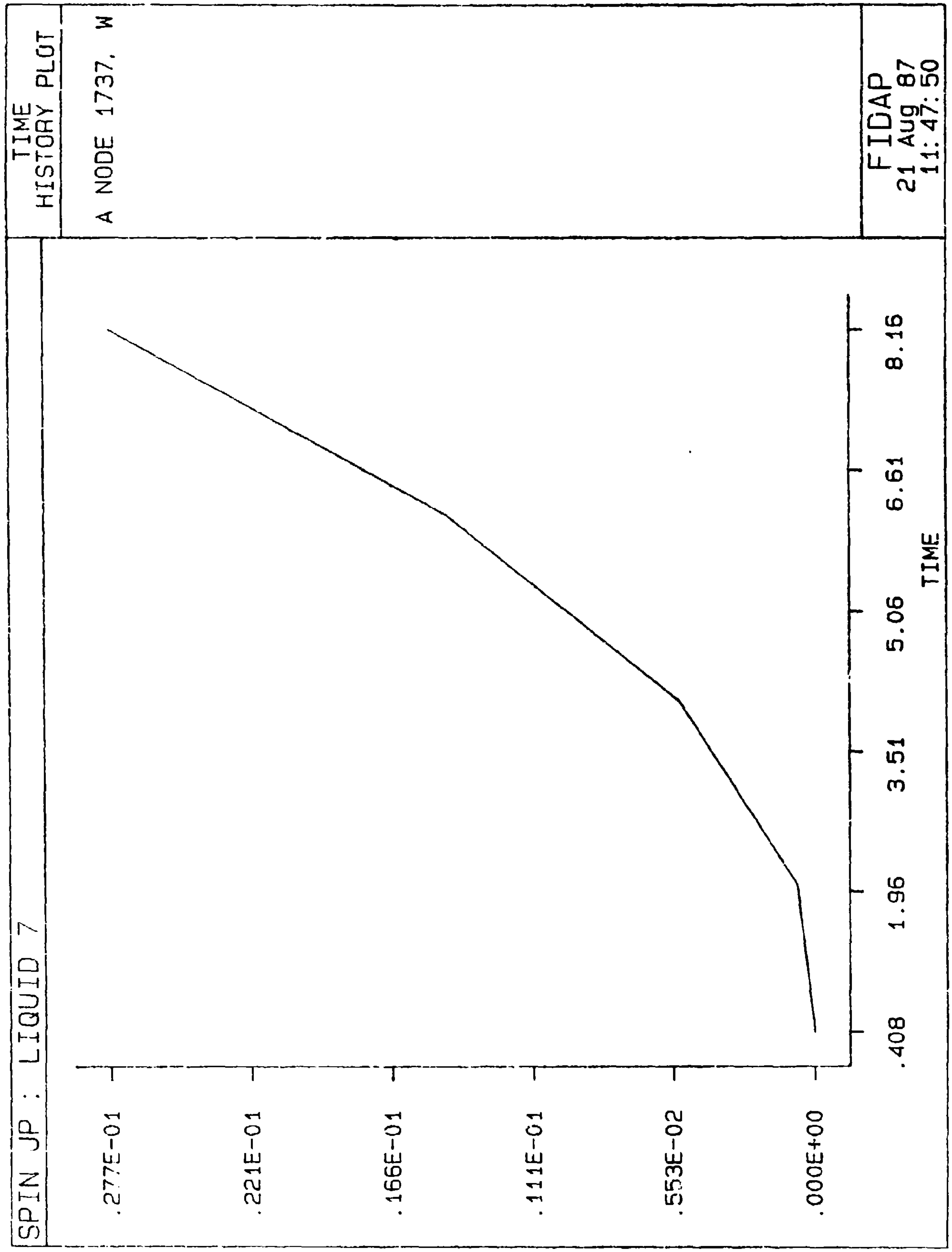

TIME
HISTORY PLOT
A NODE 1737, W
FIDAP
21 Aug 87
11: 47: 50
SPIN JP : LIQUID 7
.277E-01
.221E-01
.166E-01
.111E-01
.553E-02
.000E+00
.408
1.96
3.51
5.06
6.61
8.16
TIME

Figure 13

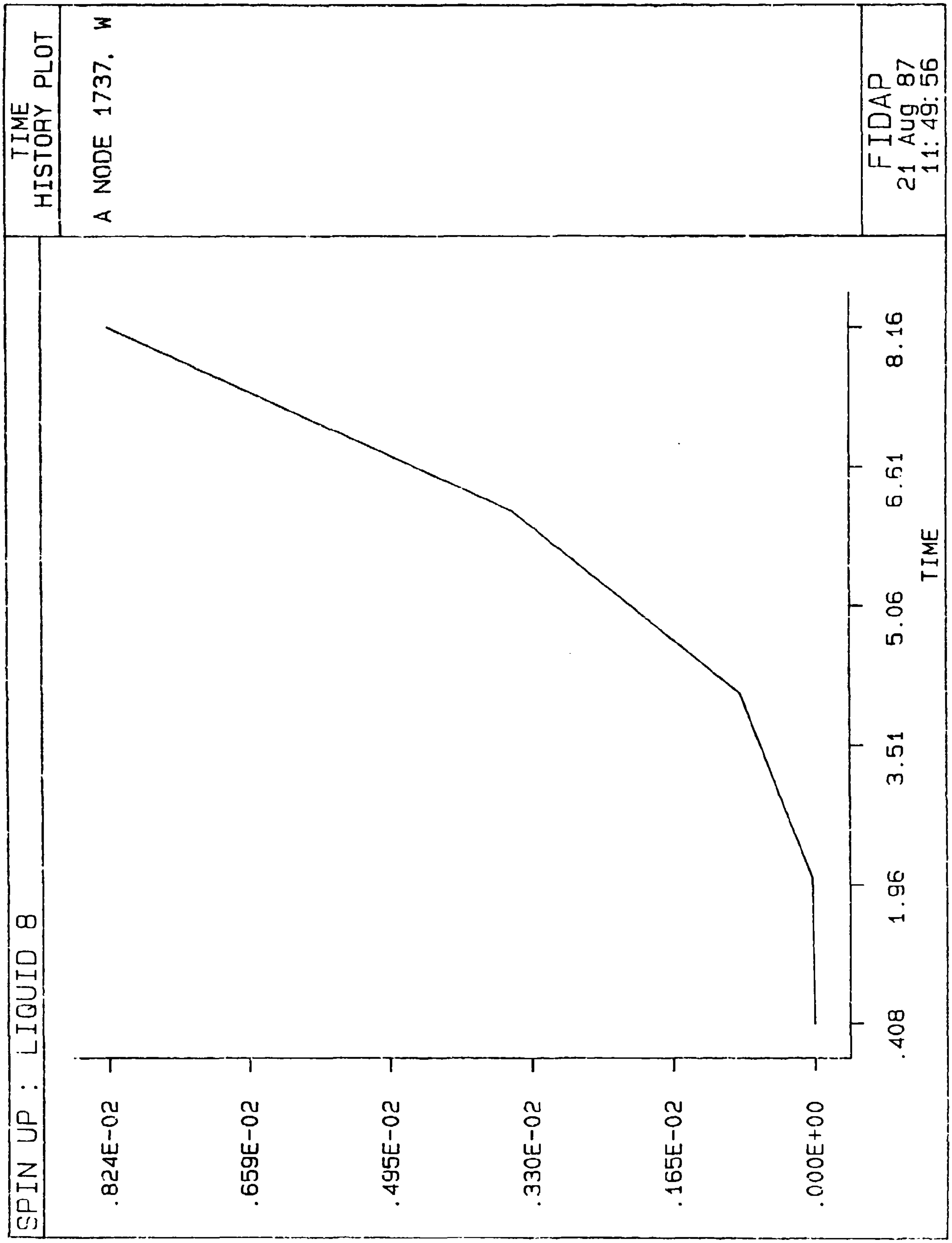
SPIN UP : LIQUID 8
TIME
HISTORY PLOT
A NODE 1737, W
FIDAP
21 Aug 87
11:49:56
.824E-02
.659E-02
.495E-02
.330E-02
.165E-02
.000E+00
.408
1.96
3.51
5.06
6.61
8.16
TIME

Part II

DESPIN MOMENT

Formulation

Computations were performed to determine the despin moment on the container described in Part I on the assumption that the liquid had become fully spun up, and that the system was moving under spin and nutation at a prescribed coning angle. The angular velocity of the spin is denoted ω and the angular velocity of the nutation is denoted Ω. The axis of the cylinder is inclined to the vertical at the coning angle θ. The two axes of rotation intersect at the midpoint of the base of the cylinder.

The problem was solved by formulating the governing equations in a nutating frame of reference, the so-called aeroballistic frame. In this coordinate system, the z-axis coincides with the axis of the cylinder, the x-axis lies in the plane containing the angular velocity vectors $\underline{\omega}$ and $\underline{\Omega}$, and the y-axis is perpendicular to this frame. This constitutes a right-handed cartesian system.

The governing equations were written in dimensionless form, with lengths, velocity, pressure, stress, strain rate and body force made non-dimensional according to the same scalings as were used in Part I. The angular velocity vector $\underline{\Omega}$ of nutation is non-dimensionalized with respect to its magnitude Ω. The governing equations for steady motion in the aeroballistic frame are then found to be

$$\underline{v}\cdot\nabla\underline{v} + 2\eta\underline{\Omega}\times\underline{v} + \eta^2\underline{\Omega}\times(\underline{\Omega}\times\underline{r}) = -\nabla p + \frac{1}{Re}\nabla\cdot\underline{T} + \underline{F} \qquad (13)$$

$$\nabla\cdot\underline{v} = 0 \qquad (14)$$

where Re is the Reynolds number defined by equation (9) and η is the spin ratio

$$\eta = \frac{\Omega}{\omega} \tag{15}$$

The dimensionless angular velocity Ω with respect to the cartesian aeroballistic frame is

$$\underline{\Omega} = -\sigma \underline{i} + \sqrt{1-\sigma^2}\ \underline{k} \tag{16}$$

where

$$\sigma = \sin\theta \tag{17}$$

is the third principal parameter of the problem.

The boundary conditions imposed for the solution of the problem were:

i) the normal velocity component is zero at all rigid boundaries;
ii) the tangential velocity at rigid boundaries is equal to the rotational velocity of that boundary;
iii) the normal velocity and the tangential stress are zero at the free surface of the liquid.

Computations and Results

Solutions were computed for six different cases: three of these related to Newtonian liquid 1*N* of Part 1, and three to non-Newtonian liquid 1. These liquids have (zero-shear-rate) viscosity of about 1000 poise and, as shown in Part 1, were both fully spun up. The various cases considered reflected the spin rate and coning rate at different instants during flight.

The quantity of interest was the despin moment denoted M_z in dimensionless form and M_z^* in dimensional form. The relation between the two, in accordance with the scaling of Part 1, is

$$M_z^* = \rho R_2^5 \omega^2 M_z$$

Once the velocity field has been computed using FIDAP, the despin moment is calculated with the aid of a simple subroutine.

The results of the computations are shown in Table 3.

Newtonian Liquid

Case #	ω rpm	Ω rpm	η spin ratio	Re	M_z	M_z^* ft-lbs
1	640	54	.0844	8.75	.000324	.0211
2	255	230	.9020	3.49	.009453	.0975
3	272	136	.5000	3.72	.003188	.0374

Non-Newtonian Liquid

Case #	ω rpm	Ω rpm	η spin ratio	Re	M_z	M_z^* ft-lbs
1	640	54	.0844	8.75	.001384	.0899
2	255	230	.9020	3.49	.044821	.4623
3	272	136	.5000	3.72	.011733	.1377

TABLE 3. Despin Moments

It is clear that the non-Newtonian liquid exerts a despin moment about four times as great as the Newtonian liquid with the same zero-shear-rate viscosity, all other parameters being equal. This can presumably be attributed to the shear thinning effects present in the non-Newtonian

liquid and the corresponding change in Reynolds number. However, as can be seen from Table 3, Reynolds number is not the only parameter contributing to variation in despin moment, so that the nonlinear modification of the velocity field in the non-Newtonian case must be regarded as a significant contributing factor to the outcome.